Free Radical Research, Vol. 35, pp. 543–554
Reprints available directly from the publisher
Photocopying permitted by license only

Chelation of Hypocrellin B with Zinc Ions with Electron Paramagnetic Resonance (EPR) Evidence of the Photodynamic Activity of the Resulting Chelate

CHUNHONG TIAN, SHANGJIE XU, SHEN CHEN, JIANQUAN SHEN, MANHUA ZHANG* and TAO SHEN

Center for Molecular Science, Institute of Chemistry, Chinese Academy of Sciences, Beijing, 100080, P.R. China

Accepted by Professor M. Dizdaroglu

(Received 25 January 2001; In revised form 19 March 2001)

Hypocrellin B (HB), a perylenequinone derivative, is an efficient phototherapeutic agent. The chelation of HB with Zinc ions (Zn^{2+}) results in a metal chelate (Zn-HB) which exhibits considerable absorption (λ_{max} = 612 nm) in the phototherapeutic window. The structure of this chelate has been characterized by UV-Vis, IR and mass spectra. The redox potentials of the Zn-HB chelate were E_{ox} = +1.1 V (*vs.* SCE) and E_{re} = −0.7 V (*vs.* SCE) as measured using the circle volt curve. The quantum yield of singlet oxygen generated by the Zn-HB chelate was 0.86, which both the electron spin trap (EPR) method and the chemical trap method show to be about 0.1 higher than that of its parent compound HB. In irradiated oxygen-saturated solutions of Zn-HB chelate, superoxide radical anions and hydroxyl radicals were detected by EPR spectroscopy using 5,5-dimethyl-1-pyrroline-*N*-oxide (DMPO) as the spin-trapping agent.

Keywords: Hypocrellin B; Zinc ion; Chelate; Electron paramagnetic resonance; Photodynamic activity; Singlet oxygen

INTRODUCTION

Photodynamic therapy (PDT) has received increasing attention in recent years as a new method for selective treatment of solid tumors.[1] Although the tumor cure mechanism is likely to require the interplay of several biological responses, a key point remains the ability of the photosensitizing agent to be retained to some extent by the tumor and, upon absorption of light to generate short-lived toxic species, in particular singlet oxygen. Hypocrellins, natural perylenequinonoid pigments, including hypocrellin A (HA) and hypocrellin B (HB) (Fig. 1), have been proposed as potential second-generation photosensitizers for PDT.[2–4] These perylenequinonoid compounds have been used as phototherapeutic agents for various skin diseases and superficial tumors, and have been

*Corresponding author. Institute of Photographic Chemistry, Chinese Academy of Sciences, Beijing, 100101, P.R. China. Fax: +86-10-6487-9375. E-mail: g214@ipc.ac.cn

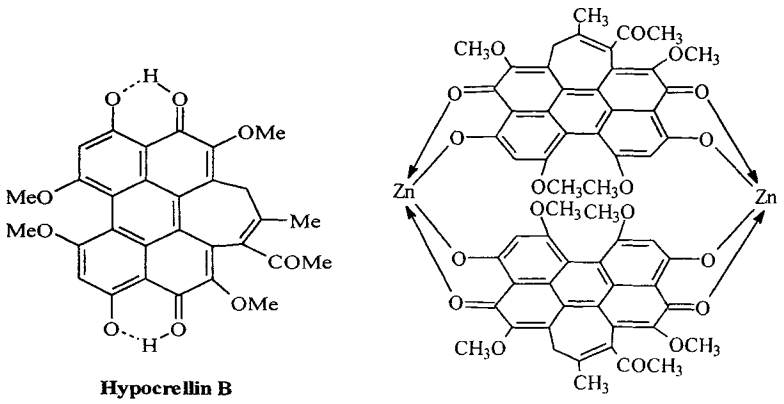

FIGURE 1 Hypocrellin B structure and proposed Zn-HB chelate structure.

taken orally as folk medicine for several centuries in China.[5] In addition, hypocrellins have been reported to display photoinduced antiviral activities against the human immunodeficiency virus (HIV-1), herpes simplex virus Type I, Sindbis virus, and vesicular stomatitis (VSV) with the involvement of singlet oxygen, i.e. the Type II mechanism.[6–9]

The chelation of HA with the II A metal ions has been investigated in recent years.[10,11] The results showed that the hypocrellins–metal complexes possess similar photochemical, photophysical and phototherapeutic properties to their parent compounds. Although the complexes have some qualities that are better than hypocrellins such as bathochromic shift of the absorption and higher water solubility, they have shortcomings that may restrict their application in PDT. For example, they are unstable and may decompose to HA in solution.[10] Using Al^{3+} as the chelation metal[12] improves the stability of the chelate, but may cause some harmful effects.

To improve the absorption in the phototherapeutic window (600–900 nm) of the hypocrellins, HB was chelated with zinc ion. The photosensitizing activity of the Zn-HB chelate was then evaluated using electron paramagnetic resonance (EPR) and spectro-photometric measurements to investigate the photosensitization mechanism.

MATERIALS AND METHODS

Materials

Lithium perchlorate ($LiClO_4$) was purchased from Merck and then dried for 12 h at 200°C before use. 5,5-Dimethyl-1-pyrroline-*N*-oxide (DMPO) was purchased from the Aldrich Chemical Company (Milwaukee, WI, USA). 2,2,6,6-Tetramethyl-4-piperidone (TEMP), 2,2,6,6-Tetramethyl-4-piperidone-*N*-oxyl radical (TEMPO), *p*-benzoquinone and 9,10-diphenyl anthracene (DPA) were also obtained from the Aldrich Chemical Company. 1,4-Diazabicyclo [2,2,2] octane (DABCO) and dimethylsulfoxide (DMSO) were purchased from the Merck Chemical Company (Darmstadt, Germany). Superoxide dismutase (SOD), reduced glutathione (GSH) and reduced nicotinamide adenine dinucleotide (NADH) were obtained from the Biotech Technology Corporation, Chinese Academy of Sciences (Beijing, China). Zinc chloride, deuterated solvents, ethanol, *N,N*-dimethylformamide (DMF) and other reagents of analytical grades were purchased from the Beijing Chemical Plant (Beijing, China).

Crude HA was prepared by acetone extraction of *Hypocrella bambusae* (B. et Br) *Sacc.* The lipids were removed by counter extraction with petroleum ether. Further purification was carried out on a silica gel column, followed by 1%

potassium dihydrogen phosphate-silica gel thin-layer chromatography and recrystallization from acetone twice. HB was prepared by quantitative potassium hydroxide dehydration of HA, followed by neutralization with 10% hydrochloric acid, chloroform extraction evaporation under reduced pressure and recrystallization from benzene-petroleum ether.

Preparation of the Chelate

200 mg of HB (379 mmol) and reductant $ZnCl_2$ were stirred in $CHCl_3$. After 10 min, the mixture was filtered. The filtrate was evaporated to dryness under high vacuum. The residue obtained was re-dissolved in ethanol and dialysed against distilled water (or ethanol) using membrane tubing (Spectrapor). After dialysis, the solution was dried under vacuum to obtain the desired Zn-HB chelate.

Methods

Absorption spectra were recorded with a Shimadzu UV 160A UV-Vis spectrophotometer. Fluorescence spectra were recorded with a Hitathi MPF 4F spectrofluorimeter. Infrared spectra were recorded with a Perkin–Elmer 983 grating spectrophotometer. Mass spectrum was recorded with a Bruker BIFLEX III matrix assisted laser desorption/ionization time of flight mass spectrograph.

Electrochemical measurements were carried out in 0.1 mol dm^{-3} solution of $LiClO_4$ in DMF at 25°C in a three-electrode measuring cell. Platinum flat with 0.8 mm diameter was used as the working electrode with a platinum wire used as the counter electrode. A NaCl-saturated calomel electrode was used as the reference electrode. The sweep rate was 45-mV s^{-1}. The DMF was dried and redistilled before use. All measurements were carried out using a Model 551-potentiostat and a 3036 XY recorder.

EPR spectra were obtained at room temperature (22–24°C) using a Bruker ESP-300E spectrometer operating at 9.8 GHz, X-band with 100 kHz field modulation (Faellanden, Switzerland). Photoinduced EPR spectra were obtained from the samples (40 μl) injected into quartz capillaries designed specially for EPR analysis. Anaerobic samples were made in cuvettes that allowed purging of the reactive volume with argon for 30 min in the dark. The samples were immediately transferred to quartz capillaries under argon. EPR spectra were recorded, stored and manipulated using an IBM/PC computer. In the DMPO spin trapping experiments, the sample irradiations were performed inside the microwave cavity as described previously.[13] A YAG-900 laser (532 nm) was used (Spectro-Physics Lasers, Mt. View, CA, USA) with an intensity of 100 mW cm^{-2} and a fluence of 20 J cm^{-2}. The spectrum factor and hyperfine splitting constants for the spin adduct could be used to infer the existence of $O_2^{\cdot-}$ and $^{\cdot}OH$.[14] TEMP was also used as a spin trap to trap singlet oxygen as proposed by Lion.[15]

The quantum yields of $^1O_2$-generation by the photosensitization were determined by DPA-bleaching methods as well as TEMP spin trapping. The details of the DPA-bleaching method were described in an earlier report.[16] A medium-pressure mercury vapor lamp (450 W) was used as the light source. An interference filter of 516 nm was used to isolate the 516 nm emission wavelength of the lamp. The reactions were followed spectrophotometrically by observing the decrease in the 374 nm absorption peak of 9,10-DPA (where the sensitizers have the lowest absorptivity) as a function of irradiation time. Lower concentrations of photosensitizer (50–70 μM) were used to reduce the autoquenching effect which occurs at higher concentrations.

The efficiencies of the free radicals and the active oxygen species generation by the Zn-HB chelate and the HB were compared by comparing their absorbance at 532 nm with identical illumination conditions. The ratio of the molar extinction coefficients at 532 nm: 4164 for HB, 2577 for Zn-HB complex, gave the

concentration ratio of HB and the Zn-HB complex as 0.63:1.

RESULTS AND DISCUSSION

Chelation of HB with Zinc Ions

The absorption spectrum of HB in ethanol was shown in Fig. 2, the maxima in the visible region were at 467, 535 and 584 nm. The addition of $ZnCl_2$ led to a red shift and an increase in the visible absorption of HB (Fig. 2) which implies the chelation of HB with Zn^{2+}. The absorption maxima of the chelate in the visible region were at 485 nm ($\varepsilon = 13877\ l\,mol^{-1}\,cm^{-1}$) and 612 nm ($\varepsilon = 6542\ l\,mol^{-1}\,cm^{-1}$). Only one group of isosbestic points at 470, 505 and 590 nm were observed within the examined spectral region (400–700 nm), indicating that the reaction produced a single chelate.

The fluorescence excitation spectra of HB and the HB–Zn chelate are shown in Fig. 3. The Zn-HB spectrum has three bands (490, 570 and 615 nm) which differed from those of HB (470, 550 and 580 nm), also indicating that a chelate was produced.

Figure 4 shows the IR spectra of HB (Fig. 4(a)) and the chelate (Fig. 4(b)). HB shows two C=O bonds in $v = 1691\,cm^{-1}$ (acetyl group) and $1611\,cm^{-1}$ (quinonoid carbonyl group).[11] In the chelate, the bands are broadened and the band at $1611\,cm^{-1}$ shifted to $1593\,cm^{-1}$ ($\Delta v = 18\,cm^{-1}$), suggesting that coordination of HB takes place via the quinonoid carbonyl oxygen.

The results obtained from the UV-Vis, IR and mass spectra were used to propose a probable structure (Fig. 1) for the chelate. Similar structures have been proposed for HA chelates with some non-transition metal ions[17] and Cu^{2+}.[18] Since none of the formula weights of these chelates have been reported, matrix assisted laser desorption/ionization time of flight mass spectrum were used to determine the molecular weight of the Zn-HB chelate with 1183 recorded as the molecular ion peak, which confirmed that the chelate in Fig. 1 was obtained.

The Zn-HB chelate is soluble in polar organic solvents, such as DMF and DMSO. Exposure of the chelate to UV-Vis light for a long time at room temperature does not markedly change its absorption spectrum, indicating that the

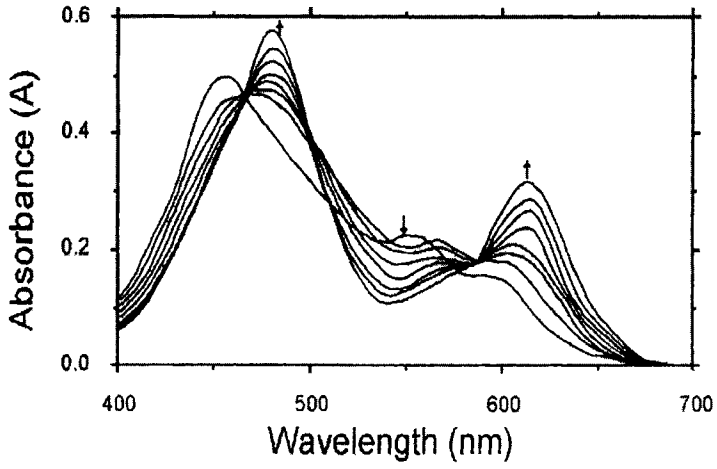

FIGURE 2 Changes in the absorption spectrum obtained by adding various amounts of Zn^{2+} to an ethanol solution of HB (5×10^{-5} M). Arrows indicate the directions of the changes.

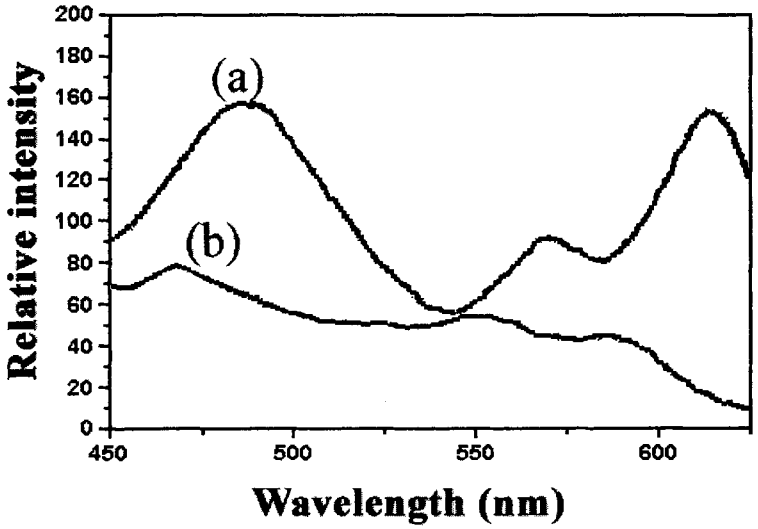

FIGURE 3 Fluorescence excitation spectra of HB (a) and Zn-HB chelate (b). The excitation wavelength was 650 nm.

chelate has high photochemical stability in neutral media. However, at higher temperatures (above 70°C), the Zn-HB absorption spectrum changes significantly due to the demethylation of the methoxy groups in the Zn-HB chelate.[19]

Electrochemical Study of the Resulting Zn-HB Chelate

Circle volt curves of HB and the Zn-HB chelate showed well separated, diffusion controlled monoelectronic cathodic waves with the peak

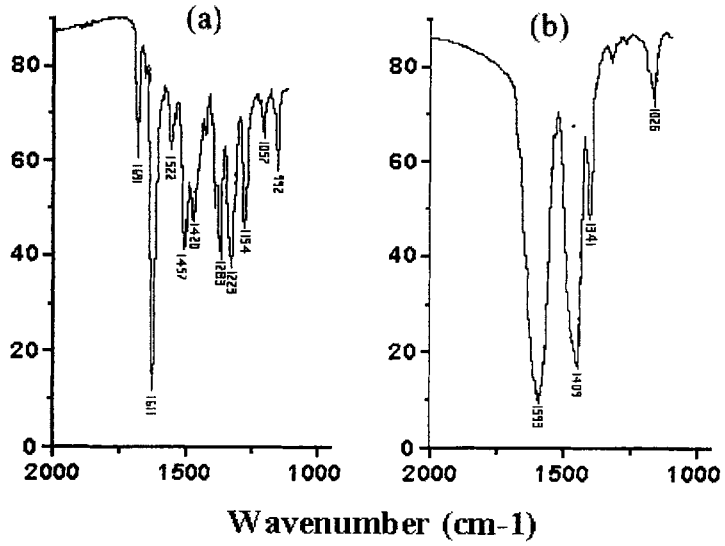

FIGURE 4 IR absorption spectra in the region 2000–1000 cm^{-1} for HB (a) and Zn-HB chelate (b) as KBr discs.

corresponding to the one-electron reduction of the compound to the semiquinone anion radical.

$$HB + e \rightleftharpoons HB^{\cdot -} \quad (1)$$

$$Zn\text{-}HB + e \rightleftharpoons [Zn\text{-}HB]^{\cdot -} \quad (2)$$

The redox potentials are listed in Table I. As shown, HB and the chelate exhibited similar oxidation potentials but quite different reduction potentials. The reduction potential of the Zn-HB chelate was more negative than that of HB, meaning that Eq. (1) proceeded more easily than Eq. (2),[20] i.e. HB obtains an electron more easily than the Zn-HB chelate.

TABLE I Redox potentials of HB and Zn-HB chelate. (*vs.* SCE)

	E_{ox}*	E_{re}†
HB	+1.10	−0.53
Zn-HB	+1.10	−0.70

* Oxidation potentials
† Reduction potentials

EPR Measurements of Free Radicals Produced During Anaerobic Photosensitization of Zn-HB

Illumination of Zn-HB (5 mM) in an argon gassed DMF solution for 1 min induced the generation of a strong EPR signal as shown in Fig. 5.

No EPR signal was observed in the absence of the photosensitizer or illumination. The signal intensity increased rapidly with the Zn-HB concentration (inset in Fig. 5). The EPR signal intensity increased rapidly during irradiation (Fig. 6) and decreased slowly in the dark. Exposure of the sample to oxygen quenched the EPR signal (Fig. 5(c)). The strong concentration effect indicates that the Zn-HB anion signal might be induced by self-electron transfer between the ground and excited species, similar to hypocrellins and some of their derivatives[21–23] and that a similar mechanism is involved (Eq. 3).

$$^3[Zn\text{-}HB] + [Zn\text{-}HB] \rightarrow [Zn\text{-}HB]^{\cdot -} + [Zn\text{-}HB]^{\cdot +} \quad (3)$$

In general, the quinone radical cation is difficult to detect in common organic solvents owing to its strong oxidizing ability. Therefore, the radical cation should be detected in solvents with high ionization potential such as Freon-113[24] at low temperature so that the signal may be ascribed to the semiquinone anion radical of the Zn-HB chelate. The following experiments were performed to identify the signals in Fig. 5. (a) Zn-HB (0.5 mM) in de-aerated DMF solution was illuminated for 1 min in the presence of NADH (5 mM), a typical electron donor (D). The EPR spectrum (Fig. 5(b)) was very similar to that observed in the absence of NADH (Fig. 5(a)) except that the addition of NADH significantly intensifies the EPR signal which indicates the anionic character of the radical. (b) A series of other electron donors, such as cysteine, GSH and ascorbic acid, were used instead of NADH, with similar results. These reductants, more electron-rich than Zn-HB, may donate an electron directly to the excited Zn-HB to form $[Zn\text{-}HB]^{\cdot -}$ (Eq. 4):

$$^3[Zn\text{-}HB] + D \rightarrow [Zn\text{-}HB]^{\cdot -} + D^{\cdot +} \quad (4)$$

(c) The $[Zn\text{-}HB]^{\cdot -}$ signal was quenched significantly by oxygen, with the signal disappearing completely when oxygen was bubbled through the Zn-HB solution (Fig. 5(c)). Furthermore, with DMPO and oxygen present in the Zn-HB solution, the EPR signal of the DMPO-superoxide radical adduct was detected immediately, accompanied by a significant decrease or disappearance of the Zn-HB EPR signal (Eq. 5):

$$[Zn\text{-}HB]^{\cdot -} + O_2 \rightarrow Zn\text{-}HB + O^{\cdot -} \quad (5)$$

In accordance with the above observations, the EPR signals shown in Fig. 6 can be safely assigned to $[Zn\text{-}HB]^{\cdot -}$. In addition, the generation efficiencies of $HB^{\cdot -}$ and $[Zn\text{-}HB]^{\cdot -}$ on illumination (Fig. 6) showed that the $HB^{\cdot -}$ generation efficiency is twice that of the $[Zn\text{-}HB]^{\cdot -}$ generation, as explained by the

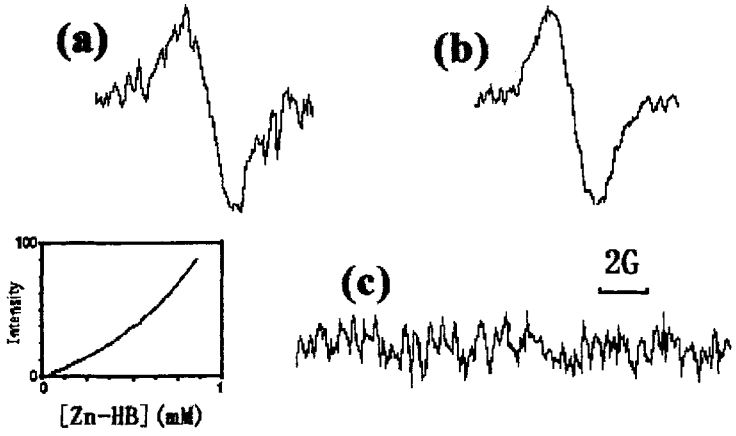

FIGURE 5 (a) Photoinduced EPR spectrum from a de-aerated DMF solution of Zn-HB (0.5 mM) on illumination (λ_{ex} = 532 nm) for 1 min. (b) Same as in (a) but in the presence of NADH (5 mM). (c) Same as in (a) but with oxygen bubbled through the solution after illumination. Inset: dependence of the relative intensity of the $[Zn\text{-}HB]^{\cdot -}$ EPR signal on the Zn-HB concentration ([Zn-HB]). Instrument settings: microwave power, 8 mW; modulation amplitude, 0.97 G; scan width, 20 G; receiver gain, 1×10^5.

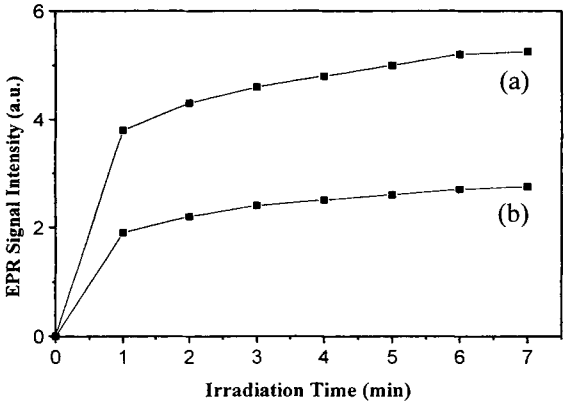

FIGURE 6 Dependence of the EPR signal intensity of $[Zn\text{-}HB]^{\cdot -}$ on irradiation time (λ_{ex} = 532 nm) by photolysis of de-aerated DMF solution containing Zn-HB (0.5 mM) (line B). Line A: Same as in line B but the Zn-HB replaced by HB (0.3 mM) (a.u., arbitrary unit). Instrument settings: microwave power, 8 mW; modulation amplitude, 0.97 G; scan width, 20 G; receiver gain, 1×10^5.

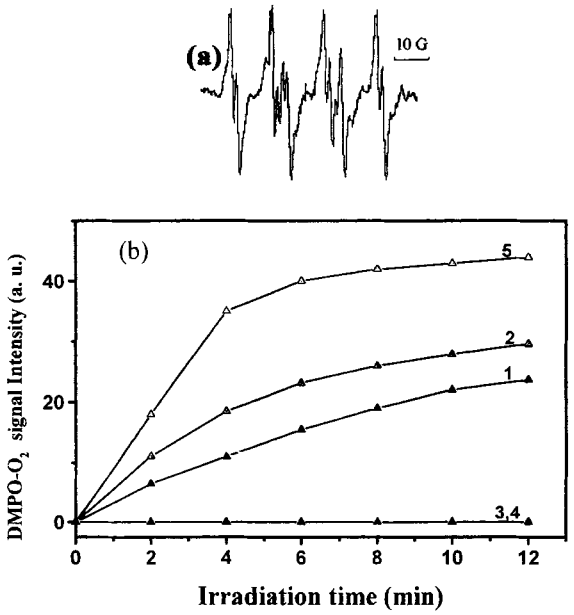

FIGURE 7 (a) EPR spectrum of DMPO-superoxide radical adduct produced from irradiation (λ_{ex} = 532 nm) of oxygen saturated DMF solution of Zn-HB (0.5 mM) and DMPO (50 mM). (b) Dependence of the DMPO-superoxide radical signal intensity on the irradiation time: line 1, for a solution of Zn-HB (0.5 mM) and DMPO (50 mM); line 2, same as line 1 but with Zn-HB replaced by HB (0.3 mM); line 3, in the absence of Zn-HB, oxygen or illumination; line 4, same as line 1 except with SOD (25 $\mu g\,ml^{-1}$) was added; line 5, same as line 1 except with NADH (4 mM) added. Instrument settings: microwave power, 8 mW; modulation amplitude, 0.97 G; scan width, 60 G, receiver gain, 5×10^4.

electrochemical study which showed that HB produced electrons more easily than the Zn-HB chelate.

Generation of Superoxide Anion Radical ($O_2^{\cdot-}$) By Zn-HB Chelate

The previous measurements showed that the photoinduced EPR signal of $[Zn\text{-}HB]^{\cdot-}$ shown in Fig. 5(a) and (c) disappeared when oxygen was bubbled through the de-oxygenated Zn-HB solution. When DMPO and oxygen were introduced into the reaction system, a new EPR signal appeared suggesting the oxidation of $[Zn\text{-}HB]^{\cdot-}$ by the dissolved oxygen and the formation of another radical that could be spin trapped by DMPO (Fig. 7(a)). This signal was characterized by three coupling constants due to the nitrogen and the two hydrogen atoms at the β and γ positions. The g factor and the determined constants ($g = 2.0056$, $a^N = 13.0\,G$, $a_\beta^H = 10.3\,G$ and $a_\gamma^H = 1.4\,G$) were in good agreement with the literature values for the DMPO-superoxide radical adduct.[25] Control experiments (Fig. 7(b), line 3) confirmed that Zn-HB, oxygen and irradiation were all necessary for production of the EPR signal shown in Fig. 7(a). The addition of SOD ($25\,\mu g\,ml^{-1}$) prior to illumination inhibited the EPR signal intensity (Fig. 7(b), line 4), whereas thermally denatured SOD had no effect on the EPR spectrum. The EPR signal was also suppressed by *p*-benzoquinone (5 mM), an efficient scavenger of $O_2^{\cdot-}$.[26] These observations support the correct assignment of the EPR signal in Fig. 7(a) to the DMPO-$O_2^{\cdot-}$ adduct.

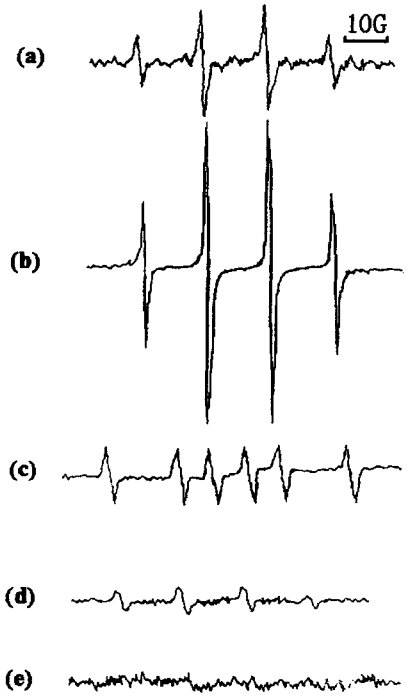

FIGURE 8 (a) EPR spectrum of DMPO-·OH adduct in oxygen saturated DMF/water ($v:v = 9:1$) solution containing Zn-HB (5×10^{-5} M) and DMPO (50 mM) irradiated ($\lambda_{ex} = 532$ nm) for 1 min; (b) same as (a) but irradiated for 2 min; (c) same as (b) except with ethanol (10 %) added; (d) same as (b) except with SOD ($40\,\mu g\,ml^{-1}$) added; (e) same as (b) except with catalase ($25\,\mu g\,ml^{-1}$) added. Instrument settings: microwave power, 8 mW; modulation amplitude, 1.54 G; scan width, 100 G; receiver gain, 1×10^5.

The addition of DABCO (10 mM) and histidine (10 mM), commonly used to inhibit $^1O_2$-dependent reactions,[27] does not reduce the EPR signal intensity of the DMPO-$O_2^{\cdot-}$ adduct, indicating that $^1O_2$ is not involved in the formation of $O_2^{\cdot-}$ by the Zn-HB chelate. The addition of electron donors, such as NADH (4 mM), GSH (5 mM) or ascorbic acid (3 mM), greatly enhanced the EPR intensity of the DMPO-$O_2^{\cdot-}$ adduct (Fig. 7(b), line 5). Control experiments ensured that no signal was obtained without light, oxygen or Zn-HB in the presence of the electron donors. The results suggest the following processes for the formation of superoxide that occurs in the absence (Eqs. 6 and 7) or presence of electron donors such as GSH (Eqs. 8 and 9):

$$^3[Zn\text{-}HB] + Zn\text{-}HB \rightarrow [Zn\text{-}HB]^{\cdot-} + [Zn\text{-}HB]^{\cdot+} \quad (6)$$

$$[Zn\text{-}HB]^{\cdot-} + O_2 \rightarrow Zn\text{-}HB + O_2^{\cdot-} \quad (7)$$

$$^3[Zn\text{-}HB] + D \rightarrow [Zn\text{-}HB]^{\cdot-} + D^{\cdot+} \quad (8)$$

$$[Zn\text{-}HB]^{\cdot-} + O_2 \rightarrow [Zn\text{-}HB] + O_2^{\cdot-} \quad (9)$$

The consistent enhancement of the $O_2^{\cdot-}$ formation by the electron donors with [Zn-

HB]$^{\cdot -}$ suggests that [Zn-HB]$^{\cdot -}$ could be the precursor for the formation of $O_2^{\cdot -}$. The efficiencies of $O_2^{\cdot -}$ generation by HB and the Zn-HB chelate, Fig. 7, shows that the HB efficiency was higher than that of Zn-HB, which agrees with the electrochemical results.

Transformation of $O_2^{\cdot -}$ into $^{\cdot}OH$

The DMPO spin-trap method has been successfully applied to trap $^{\cdot}OH$ and $O_2^{\cdot -}$.[14,28–30] Interaction of DMPO with $^{\cdot}OH$ leads to the formation of DMPO-$^{\cdot}OH$ adduct signal with a reaction constant of approximately $2\times10^9\,M^{-1}s^{-1}$ at pH 7.0.[31]

Irradiation of an oxygen-saturated DMF/water ($v:v=9:1$) solution containing Zn-HB (5×10^{-5} M) and DMPO (50 mM) with 532 nm light produced a four-line EPR spectrum (Fig. 8(a)) with an intensity ratio of 1:2:2:1 and hyperfine coupling constants of $a^N = a^H_\gamma = 14.9$ G showing that this radical species is the DMPO-$^{\cdot}OH$ adduct.[31] The signal intensity increased with prolonged irradiation of the solution (Fig. 8(b)). When ethanol (10%, v/v) was added, the EPR signal of the DMPO-$^{\cdot}CH(OH)CH_3$ adduct with $a^N = 15.8$ G and $a^H = 23.0$ G was observed (Fig. 8(c)).[31] These results further confirm the assignment of the signal to the DMPO-$^{\cdot}OH$ radical adduct.

The formation of $^{\cdot}OH$ by Zn-HB depends on the oxygen, light, DMPO and Zn-HB concentration. To confirm whether the observed DMPO-$^{\cdot}OH$ adduct of the spin trap unequivocally proves the formation of $^{\cdot}OH$, SOD and catalase enzymes were used as probes. The addition of SOD (40 μg ml^{-1}) inhibits the formation of DMPO-$^{\cdot}OH$ adduct by over 50% (Fig. 8(d)), indicating that superoxide radical anion is involved in the formation of $^{\cdot}OH$ by Zn-HB. We have demonstrated that $O_2^{\cdot -}$ can be generated from Zn-HB by photoexcitation in the presence of oxygen (see above). In DMF/water solution, $O_2^{\cdot -}$ formed after irradiation can then undergo rapid dismutation to H_2O_2 and O_2 (Eqs. 10 and 11).

$$O_2^{\cdot -} + H^+ \rightarrow HO_2^{\cdot} \quad (10)$$

$$H_2O + HO_2^{\cdot} + O_2^{\cdot -} \rightarrow H_2O_2 + O_2 + {}^{-}OH \quad (11)$$

When catalase (25 μg ml^{-1}) was added to the DMF/water ($v:v=9:1$) solution of Zn-HB and DMPO, no EPR signal was detected after irradiation (Fig. 8(e)), confirming that DMPO-$^{\cdot}OH$ does not arise from the decomposition of DMPO-$O_2^{\cdot -}$. These results support the view that $O_2^{\cdot -}$ is involved in the formation of $^{\cdot}OH$ by Zn-HB and the later reaction is H_2O_2 dependent. Since trace amounts of transition metal ions may be present in the solution, the formation of $^{\cdot}OH$ photosensitized Zn-HB probably proceeds via the so-called Fenton reaction (Eqs. 12 and 13):

$$Fe^{3+} + O_2^{\cdot} \rightarrow Fe^{2+} + O_2 \quad (12)$$

$$Fe^{2+} + H_2O_2 \rightarrow Fe^{3+} + {}^{\cdot}OH + {}^{-}OH \quad (13)$$

The overall reaction is then (Eq. 14):

$$H_2O_2 + O_2^{\cdot -} \rightarrow {}^{\cdot}OH + {}^{-}OH + O_2 \quad (14)$$

Another possible pathway for the generation of $^{\cdot}OH$ formed by Zn-HB may result from the reaction of semiquinone radical anion with H_2O_2 (Eq. 15).

$$H_2O_2 + [\text{Zn-HB}]^{\cdot -} \rightarrow {}^{\cdot}OH + {}^{-}OH + \text{Zn-HB} \quad (15)$$

The addition of DABCO (10 mM) and histidine (10 mM), which normally act as $^1O_2$ quenchers,[31] did not reduce the EPR signal intensity of the DMPO-$^{\cdot}OH$ adduct (not shown), indicating that $^1O_2$ is not involved in the formation of DMPO-$^{\cdot}OH$.

Formation of $^1O_2$ By Zn-HB

It has been observed that $^1O_2$ is involved in many photo-oxygenations sensitized by perylenoquinone pigments[3,4] and may play the main role in

photodynamic therapy.[34–36] It has previously been reported that TEMPO, a nitroxide radical detectable by EPR, was generated from TEMP and singlet oxygen.[33]

As shown in Fig. 9(a), a spectrum having three equal-intensity lines, characteristic of a nitroxide radical, was recorded when an oxygen-saturated DMF solution of Zn-HB (5×10^{-5} M) and TEMP (20 mM) was irradiated at room temperature. This spectrum was compared with that of the radical from commercial TEMPO. The hyperfine splitting constant and g factor of the photosensitized oxidation product of TEMP by Zn-HB were identical to those of commercial TEMPO ($a^N = 16.3$, $g = 2.0056$). Further evidence to support the involvement of $^1O_2$ in the Zn-HB photosensitization process was provided by the following experiments. The presence of $^1O_2$ scavengers (histidine or NaN_3) suppressed the EPR signal (Fig. 9(b), line 3 and line 4). Analysis of the effect of deuterium on the TEMPO yield showed that the EPR signal intensity increased about eightfold when DMF was replaced by fully deuterated DMF as solvent (not shown). Similar conditions but in the absence of Zn-HB, oxygen or light did not produce TEMPO (Fig. 9(b), line 5). All of the results suggest that TEMPO is derived from the reaction of TEMP with $^1O_2$ generated by energy transfer from excited triplet-state of Zn-HB to ground state molecular oxygen (Eq. 16).

$$^3[\text{Zn-HB}] + O_2 \rightarrow \text{Zn-HB} + {}^1O_2 \qquad (16)$$

To investigate further the photo-production of $^1O_2$ by Zn-HB, the parent compound HB[16] was used as a reference to compare the photogeneration quantum yield to TEMPO from TEMP. The TEMPO signal intensities produced in each case are proportional to their $^1O_2$-generation quantum yields (ϕ) with identical illumination of the samples at 532 nm. The previously determined $^1O_2$-generation by HB of 0.76[16] and the data in

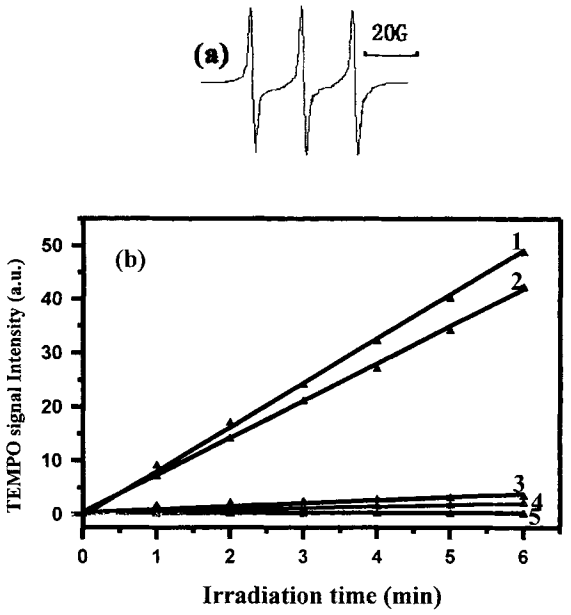

FIGURE 9 (a) EPR spectrum of TEMPO formed during irradiation (λ_{ex} = 532 nm) of oxygen saturated DMF solution containing Zn-HB (5×10^{-5} M) and TEMP (20 mM) using 532 nm light. (b) EPR signal intensity of TEMPO as a function of irradiation time (line 1); Line 2, same as line 1 except that the Zn-HB was replaced by HB (3×10^{-5} M); line 3, same as line 1 except NaN_3 (10 mM) added; line 4, same as line 1 except with histidine (1 mM) added; line 5, same as line 1 except that Zn-HB, oxygen or illumination was omitted. Instrument settings: microwave power, 8 mW; modulation amplitude, 0.97 G; scan with, 100 G; receiver gain, 1×10^5.

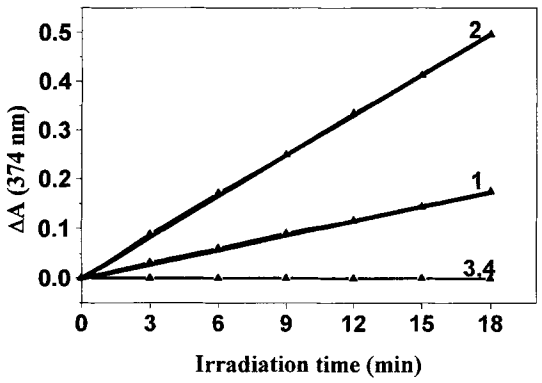

FIGURE 10 Photosensitized DPA-bleaching by measuring the absorbance decrease (Δ A) at 374 nm as a function of irradiation time (λ_{ex} = 516 nm) for an oxygen-saturated DMF solution of Zn-HB (5×10^{-5} M) and DPA (0.5 mM) (line 1); Line 2, same as line 1 except with Zn-HB replaced by HB (3×10^{-5} M); Line 3, same as line 1 except that Zn-HB, oxygen or illumination was omitted; Line 4, same as line 1 except with DABCO or histidine (5 mM) added.

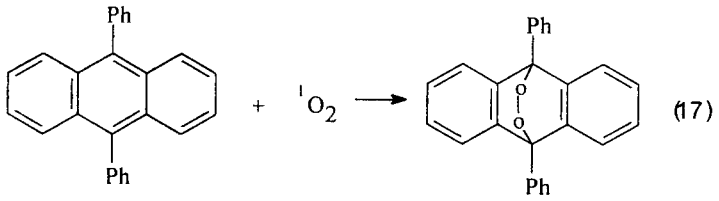

(17)

Fig. 9 were used to determine the $^1O_2$-generation quantum yield of Zn^{2+}-HB as 0.86.

In addition, the photo-oxidation of DPA to its endo-peroxide derivative by singlet oxygen (Eq. 17) was used to detect $^1O_2$ and to determine the quantum yield of $^1O_2$ formed from photosensitization using HB as a reference.[16] During the sample measurements, the absorbances at 516 nm were adjusted to be the same. Figure 10 shows the rates of DPA-bleaching photosensitized by Zn-HB and HB as a function of irradiation time at 516 nm oxygen-saturated DMF. Control experiments indicated that no DPA-bleaching occurred when Zn-HB (or HB), oxygen or irradiation was omitted (Fig. 10, line 3). The addition of DABCO or histidine (5 mM) completely inhibited DPA-bleaching (Fig. 10, line 4). These results show that DPA bleaching results from the reaction of DPA with $^1O_2$ formed by Zn-HB (or HB) photosensitization. The $^1O_2$-generating quantum yield of Zn-HB was estimated to be 0.86, using that of HB (0.76) as a reference.

CONCLUSION

A novel derivative of hypocrellin, Zn-HB chelate, with a considerable absorption at 612 nm was obtained and characterized by UV, IR, and mass spectrum. The mechanism of active oxygen species generation by Zn-HB was investigated using both an electron spin trap and a chemical trap. The quantum yield $^1O_2$ generation by Zn-HB was 0.86, which is higher than that of HB (0.76). The results imply that the Zn-HB chelate is a potential photodynamic therapeutic agent.

Acknowledgements

Financial supports from National Nature Science Foundation of China—No. 39830090 and No. 29772035—are gratefully acknowledged.

References

[1] Kessel, D. (1994) Photodynamic Therapy of Neoplastic Disease (CRC Press, Boston, MA).
[2] Jiang, L.J. (1990) "The structures, properties, photochemical reaction and reaction mechanisms of hypocrellins (I)", *Kexue Tongbao* **21**, 1608–1616.
[3] Jiang, L.J. (1990) "The structures, properties, photochemical reactions abd reaction mechanisms of hypocrellins (II)", *Kexue Tongbao* **22**, 1681–1690.
[4] Miller, G.G., Brown, K., Ballangrud, M., Barajas, O., Xiao, Z., Tulip, J., Lown, J.W., Leithoff, J.M., Allalunis-Turner, M.J., Mehta, R.D. and Moore, R.B. (1997) "Preclinical assessment of hypocrellin B and hypocrellin B derivatives for photodynamic therapy of cancer: progress update", *Photochemistry and Photobiology* **65**, 714–722.
[5] Diwu, Z.J. (1995) "Novel therapeutic and diagnostic applications of hypocrellins and hypericins", *Photochemistry and Photobiology* **61**, 529–539.
[6] Hudson, J.B., Zhou, J., Chen, J., Harris, L., Yip, L. and Towers, G.H.N. (1994) "Hypocrellin from Hypocrella bambusae, is phototixic to human immunodeficiency virus", *Photochemistry and Photobiology* **60**, 253–255.
[7] Fehr, M.J., Carpenter, S.L., Wannemuehler, Y. and Petrich, J.W. (1995) "Roles of oxygen and photoinduced acidification in the light-dependent antiviral activity of hypocrellin A", *Biochemistry* **34**, 15845–15848.
[8] Hudson, J.B., Imperial, V., Haugland, R.P. and Diwu, Z.J. (1997) "Antiviral activities of photoactive perylenequinones", *Photochemistry and Photobiology* **65**, 352–354.
[9] Hirayama, J., Ikebuchi, K., Kamo, N. and Sekiquchi, S. (1997) "Photoinactivation of virus infectivity by hypocrellin A", *Photochemistry and Photobiology* **66**, 697–700.
[10] Ma, J.N. (1988) "Studies on the photochemical and photophysical properties of hypocrellin A" PhD dissertation (Institute of Photographic Chemistry, Academia Sinica, Beijing).
[11] Diwu, Z.J., Zhang, C.L. and Lown, J.W. (1992) "Photosensitization of anticancer agents 13. The production singlet oxygen by metal-ion-chelated perylenequinones", *Journal Photochemistry and Photobiology A: Chemistry* **66**, 99–112.
[12] Hu, Y.Z., An, J.Y. and Jiang, L.J. (1994) "Studies on the chelation of hypocrellin A with aluminium ion and the

photodynamic action of the resulting complex", *Journal Photochemistry and Photobiology B.: Biology* **22**, 219–227.
[13] Hadjur, C., Jeunet, A. and Jardon, P. (1994) "Photosensitized by hypericin: ESR evidence for singlet oxygen and superoxide anion radicals formation in an *in vitro* model", *Journal Photochemistry and Photobiology B.: Biology* **26**, 67–74.
[14] Harbor, J.R. and Hair, M.L. (1978) "Detection of superoxide ions in nonaqueous media. Generation by photolysis of pigment dispersions", *The Journal of Physical Chemistry* **82**, 1397–1399.
[15] Lion, Y., Dlemelle, M. and New, A. (1976) "Method of detecting singlet oxygen production", *Nature* **263**, 442–443.
[16] Diwu, Z.J. and Lown, J.W. (1992) "Photosensitization with anticancer agents 12. Perylenequinonoid pigments, a novel type of singlet oxygen sensitizer", *Journal Photochemistry and Photobiology A: Chemistry* **64**, 273–287.
[17] Singh, H.B. and Sharma, J. (1987) "Coordination polymers of 1,4-dihydroxyanthraquinone with some non-transition metal ions: thermal, conductance and dielectric properties", *Indian Journal of Chemistry* **26A**, 167–169.
[18] Tachibana, M. and Iwaizumi, W. (1987) "EPR and UV-visible spectroscopic studies of copper (II) and cobalt (II) complexes of hydroxyanthraquinone", *Journal of Inorganic Biochemistry* **30**, 141–151.
[19] Zhao, K.H. (1989) "Studies on the structures and properties of hypocrellins" PhD Dissertation (Institute of Photographic Chemistry, Academia Sinica, Beijing).
[20] Ossowski, T., Pipka, P., Liwo, A. and Jeziorek, D. (2000) "Electrochemical and UV-spectrophotometric study of oxygen and superoxide anion radical interaction with anthraquinone derivatives and their radical anions", *Electrochimca Acta* **45**, 3581–3587.
[21] He, Y.Y., An, J.Y. and Jiang, L.J. (1999) "pH effect on the spectroscopic behavior and photoinduced generation of semiquinone anion radical of hypocrellin B", *Dyes and Pigments* **41**, 79–87.
[22] He, Y.Y., An, J.Y. and Jiang, L.J. (1998) "EPR and spectrophotometric studies on free radicals ($O_2^{\cdot-}$, Cysa-HB$^{\cdot}$−) and singlet oxygen ($^1O_2$) generated by irradiation of cysteamine substituted hypocrellin B", *International Journal of Radiation Biology* **74**(5), 647–654.
[23] Hu, Y.Z., An, J.Y., Jiang, L.J. and Chen, D.W. (1995) "Spectroscopic study on the photoreduction of hypocrellin A: generation of semiquinone anion radical and hydroquinone", *Journal Photochemistry and Photobiology A: Chemistry* **89**, 45–51.
[24] Mayer, J. and Krasluklanis, R. (1991) "Absorption spectra of the radical ions of quinones: a pulse radiolysis study", *Journal of the Chemical Society Faraday Transfer* **87**, 2943–2947.
[25] Lang, K., Wagnerova, M., Stopka, P. and Dameran, W. (1992) "Reduction of dioxygen to superoxide photosensitized by anthraquinone-2-suphonate", *Journal of Photochemistry and Photobiology A: Chemistry* **67**, 187–195.
[26] Manring, L.E., Kramer, M.K. and Foote, C.S. (1984) "Interception of $O_2^{\cdot-}$ by benzoquinone in cyanoaromatic sensitized photooxygenations", *Tetrahedron Lettters* **25**, 2523–2526.
[27] Lissi, E.A., Encinas, M.V., Lemp, E. and Rubio, M.A. (1993) "Singlet oxygen bimolecular processes. Solvent and compartmentalization effects", *Chemical Reviews* **93**, 699–723.
[28] Hadjur, C., Wagnieres, G., Ihringer, F., Monnier, P. and van de Bergh, H. (1997) "Production of the free radicals ($O_2^{\cdot-}$ and $^{\cdot}OH$) by irradiation of the photosensitizer zinc (II) phthalocyanine", *Journal of Photochemistry and Photobiology B: Biology* **38**, 196–202.
[29] Hadjur, C. and Jeunet, A. (1995) "EPR evidence of superoxide anion radicals by irradiation of a PDT photosensitizer: hypericin", In: Favier, A., Kalyanaramah, B., Cadet, J., Fontecave, M. and Pierre, J.L., eds, Methods in molecular biology (Birkhauser Verlag, Basel), pp. 119–126.
[30] Viola, A., Hadjur, C., Jeunet, A. and Julliard, M. (1996) "Electron paramagnetic resonance of generation of superoxide ($O_2^{\cdot-}$ and hydroxyl radicals ($^{\cdot}OH$) by irradiation of a new photodynamic therapy photosensitizer, victoria blue BO", *Journal Photochemistry and Photobiology B: Biology* **32**, 49–58.
[31] Finkelstein, E., Rosen, G.M. and Rauchman, E.J. (1980) "Spin trapping of superoxide and hydroxyl radical: practical aspects", *Archives of Biochemistry Biophysics* **200**, 1–16.
[32] Feix, J.B. and Kalyanaraman, B. (1991) "Production of singlet oxygen-derived hydroxyl radical adduct during merocyanine-540-mediated photosensitization: analysis by ESR-spin trapping HPLC with electron chemical detection", *Archives of Biochemistry Biophysics* **291**, 43–51.
[33] Lion, Y. and Van De Vorst Delmelle, M.A. "New method of detecting singlet oxygen production", *Nature*, **263**, 442–443.
[34] Patterson, M.S., Madsen, S.J. and Wilson, B.C. (1990) "Experimental tests of the feasibility of singlet oxygen luminescence monitoring *in vivo* during photodynamic therapy", *Journal of Photochemistry and Photobiology B: Biology* **5**, 69–84.
[35] Diwu, Z.J. and Lown, J.W. (1989) "Hypocrellins and their use in photosensitization", *Photochemistry and Photobiology* **52**, 609–616.
[36] Senthil, V., Jones, L.R., Senthil, K. and Grossweiner, L.I. (1994) "Hypericin photosensitization in aqueous model systems", *Photochemistry and Photobiology* **59**, 40–47.